*IFSCC 2025 full paper (**IFSCC2025-1039**)*

"How Carbonylation Causes Protein Discoloration: The Role of Oligomers"

Min FU[1*], Xiangyan SHI[3*], Liwei ZHANG[1*], Mengyang Xu[3*], Zhao ZHAO[1], Yang LIU[1], Jie QIU[1], Wei LI[1], Wei GU[1], Aude FOUCHER[2], Peggy SEXTIUS[2], Sandra DEL BINO[2], Helene ZUCCHI[2], Ping WANG[1#]

Affiliation:

1. L'Oréal Research and Innovation, 550 Jin Yu Road, Pudong, Shanghai, P.R. China.
2. L'Oréal Research and Innovation, 1 Avenue Eugene Schueller, 93601, Aulnay-sous-Bois, France.
3. Department of Biology, Shenzhen MSU-BIT University, International University Park Road, Dayun New Town, Longgang District, Shenzhen, Guangdong Province, 518172, P.R. China.

* These authors contributed equally to the work

Corresponding author: Ping.Wang@loreal.com

1. Introduction

Skin aging yellowness, normally characterized by increased b* value in colorimetric measurements, represents a growing cosmetic concern—particularly in cultures prioritizing bright complexions [1-3]. Besides melanin as a classical contributor to skin tone, oxidative modification of protein was also suspected as a contributor to skin aging including skin tone alteration[4-6]. While early theories implicated systemic factors (e.g., beta-carotene, bilirubin) [7-9], evidence recently points to aldehydes, or carbonyl products from lipids, as the primary driver of protein biochemical alterations during aging.

Photo-oxidation of skin lipids (e.g. squalene) generates reactive aldehydes—malondialdehyde (MDA), 4-hydroxynonenal (4-HNE), and acrolein—that form covalent adducts with epidermal proteins [10-12], these carbonylated proteins accumulate with age, correlating with dermal yellowish discoloration. However, the exact chromophores and their relationship to protein structural and colorimetric changes remain unclear. While recent studies suggest a potential role for Advanced Glycation End-products (AGEs) and matrix-integrated adducts in this multi-factorial aging process, the underlying mechanisms remain elusive.[13-17]. Further investigation is needed to elucidate these mechanisms and provide more definitive evidence. This study investigated reactive aldehydes-driven protein modifications as a key mechanism of skin yellowness. Using the B1 domain of streptococcal IgG-binding protein (GB1) —a model system with well-defined mutants (K28C, T53C)—we analyzed site-specific adduct formation

via NMR spectroscopy and correlated structural changes with chromatic shifts. Findings were then validated in a 3D skin model, with identified actives.

2. Materials and Methods

2.1 Inactive skin model preparation and treatment

3D reconstructed human epidermis (RHE) model was purchased from Shanghai Episkin Biotechnology Co.,Ltd. The reconstructed skin model was kept at -80 ℃ freezer for at least 48 hours to inactivate cellular functions. To induce protein carbonylation, the inactive skin model was incubated with 5mM of 4-HNE (Cat. Number: ZC-65374, Shanghai ZZBIO Co.,LTD.) in PBS for 7 days at 37°C. To validate the inhibition effect of the quenchers, the inactive skin samples were incubated for 7 days at 37 °C with 5mM 4-HNE in combine with 5mM of glutathione (Sigma-Aldrich), 5mM of cystidine (Sigma-Aldrich), 5mM of histidine (Sigma-Aldrich), 5mM of L-carnosine, 5mM of N-actyl-carnosine (Sigma-Aldrich) respectively. As negative controls, models were incubated with PBS plus the solvent vehicle (1/200 DMSO from Sigma-Aldrich).

2.2 In tubo protein solution treatment

To induce protein carbonylation, 4-HNE (2mM and 10mM final concentration) was used to react with the bovine serum albumin (BSA) protein solution from Thermo Fisher (1.6mg/ml final concentration) at 37 ℃ for 12 days. Samples of BSA incubated with PBS containing the vehicle (1% DMSO) were taken as negative controls.

2.3 Colorimetric measurements of skin model samples and in tubo samples: *b* Parameter Measurement*

A scalpel with sharp edge was used to cut the epidermis part off from the skin model. Pictures were taken using a camera. Color was measured by a spectro-coloriemeter (Digieye,from VeriVide Limited, UK) and the L* and b* values that represent the lightness and yellow-blue component were obtained by the Digieye software.

Pictures of the reaction tubes were taken for visual inspection. The samples were centrifuged and the supernatant in each tube was collected for spectrum detection from 350nm to 750nm by a microplate reader (Varioskan LUX, Thermo Scientific) and the spectrum data were used to calculate the L* and b* values by optical algorithm.

2.4 Carbonylation protein and total protein quantification of in tubo samples

The supernatant of each tube was collected by centrifugation for carbonylation protein quantification. The concentration of protein carbonyl and total protein were measured by commercial assay kits (STA-310, Cell Biolabs and 23227, Thermo Fisher) following the manufactures' protocols, respectively.

2.5 SDS-PAGE protein staining of in tubo samples

The supernatant of each tube was collected by centrifugation for sodium dodecyl sulfate polyacrylamide gel electrophoresis (SDS-PAGE) analysis. The protein concentrations were determined using Bradford method. (ab119216, Abcam). The loading sample buffer (NP0007,

Invitrogen) and DTT were added into samples that were subsequently heated at 70℃ for 10 minutes. 2ug of protein for each sample was loaded. The SDS-PAGE were rub on ice for about 3h (Gels: NP0336BOX, Invitrogen. Running buffer: NP0001, Invitrogen). The gel was stained in Coomassie Blue (P0017, Beyotime) and then destained for imaging.

2.6.NMR experiments

WT GB1 was expressed using E. coli BL21 (DE3) competent cells, and K28C and T53C GB1 were expressed in E. coli Rosetta 2 cells. The plasmids carry PET-3a vector and the desired sequences encoding the proteins.

The protein samples which were prepared by standared protocol were in NMR buffer containing 92%/8% of H_2O/D_2O, 20mM of HEPES (pH 7.5), and 75 mM KCl. Liquid-state NMR experiments were conducted on a 600 MHz NMR spectrometer (Avance Neo 600 MHz, Bruker, USA) equipped with a 5 mm QCI H/P/C/N CryoProbe. ^{1}H-^{15}N HSQC experiments were performed by collecting a series of spectra at different various times after adding 10mM 4-HNE into the protein samples with or without inhibitors.

2.7 Mass spectrometry

Protein samples upon reacting with 4-HNE for different periods were buffer exchanged to water, and subsequently analyzed by Matrix Assisted Laser Desorption Ionization - Time of Flight (MALDI-TOF) to obtain the molecular weights of the reaction products.

3. Results

3.1 Protein Carbonyls are not the direct chromophore that generate yellowish color

The observation that unsaturated aldehydes induce yellowing does not establish whether carbonyls are the responsible chromophores. To investigate the underlying chemical mechanism and address this question, we conducted in tubo reactions using BSA, a commonly used protein containing 607 amino acids, as a model system. After 12 days of incubation with 10mM 4-HNE, the BSA solution exhibited a yellowish color and precipitation (Figure 1A). We monitored the dynamic changes in b* value (yellowness), soluble protein carbonyl content, and total protein concentration in the supernatant. The b* value steadily increased over time (Figure 1B). Soluble protein carbonyl content increased within the first 6 to 24 hours and subsequently decreased (Figure 1C). Total soluble protein concentration decreased continuously from the start of the experiment (Figure 1D). These results suggest that 4-HNE initially induces protein carbonylation within the first 24 hours. Subsequent reactions involving the carbonylated proteins then lead to the formation of modified protein species and precipitation. The observed yellowing appears to be a consequence of these later reactions, rather than the initial carbonylation. The decrease in total soluble protein concentration is consistent with the formation of insoluble protein aggregates. Based on these observations, we hypothesize that protein carbonylation induced by 4-HNE alters protein structure, promoting protein polymerization and aggregation.

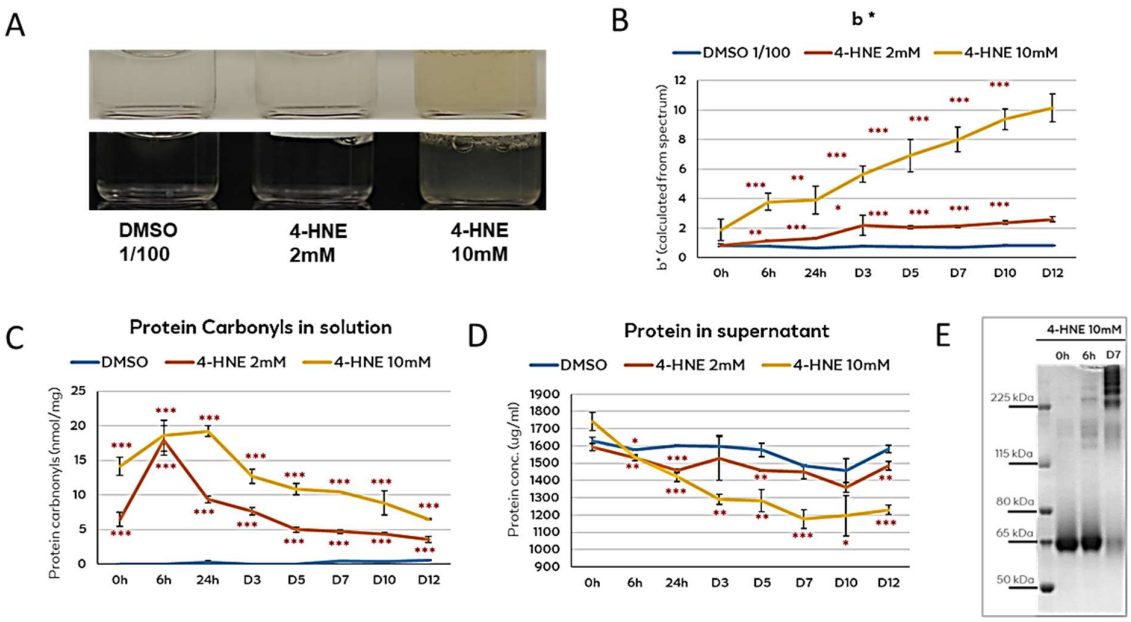

Figure 1. 4-HNE induces yellowness and precipitate in BSA protein solution (A)1.6mg/ml BSA solution react to 4-HNE for 12 days in 37°C (B) Dynamic change of b value from 0h,6h to D12 (C) Dynamic change of protein carbonyls in solution from 0h,6h to D12 (D) Dynamic change of total protein in supernatant from 0h,6h to D12 (E) SDS-PAGE image of BSA protein solution react with 4-HNE at 0h,6h and Day7 . * $p < 0.05$, ** $p < 0.01$, *** $p < 0.001$.*

SDS-PAGE analysis of the supernatant revealed minimal changes in the BSA profile over the first 6 hours, with the predominant band remaining at about 65 kDa (monomeric BSA). After 7 days, the 65 kDa band diminished substantially, and higher-molecular-weight bands (above 225 kDa) became prominent (Figure 1E), indicating the occurrence of protein polymerization.

3.2 NMR characterization suggested that 4-HNE reacting with GB1 continuously involves various residues and protein crosslinking, while the reaction kinetics depends on the reactive residue type and location.

The chemical nature of amino acid side chains dictates their susceptibility to oxidation, a phenomenon amplified under conditions of oxidative stress. Sulfur-containing residues (Met and Cys), those with aromatic rings (Phe, Tyre, and Trp), and nitrogen-rich residues (His, Lys, Agr and Pro) are particularly vulnerable. This differential reactivity influences protein folding, stability, and function, as oxidative modifications can disrupt hydrogen bonding, introduce steric hindrance, and alter electrostatic interactions. Furthermore, the location of these susceptible residues within the three-dimensional protein structure plays a significant role. Surface-exposed residues are generally more accessible to oxidants compared to those buried within the protein core, leading to a stereotypical pattern of oxidative modification.

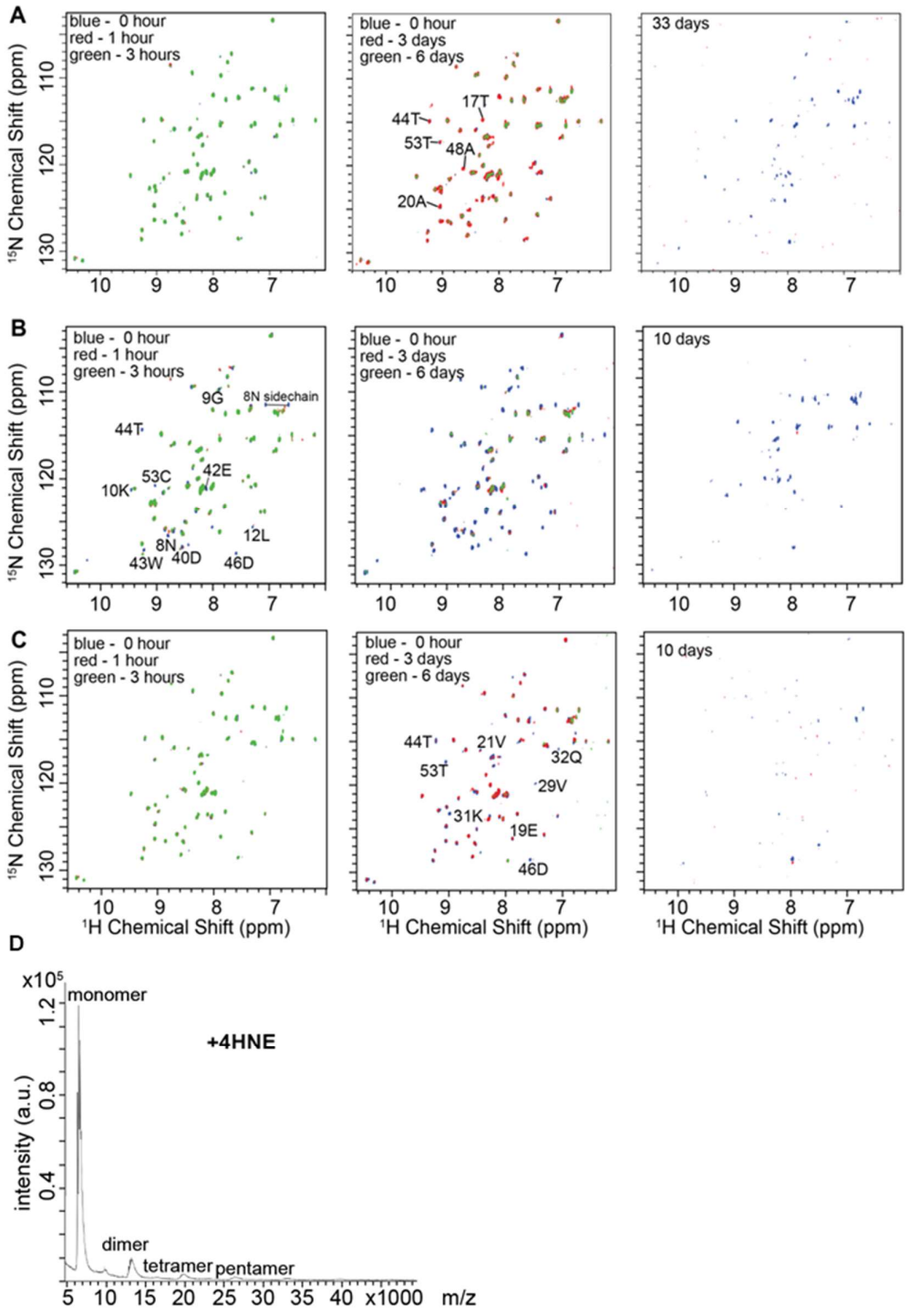

Figure 2. ^{1}H-^{15}N HSQC NMR spectra of (A) WT GB1, (B) T53C GB1 and (C) K28C GB1 reacting with 4-HNE, data were recorded at different time points as indicated in the figures. The 4-HNE concentrations were 10 mM, and the protein concentrations were 1.6 mg/ml, respectively. (D) MALDI-TOF mass spectrometry data of T53C GB1 reacting with 4-HNE for 7 days, the presence of different protein oligomers is indicated in the graphs.

To investigate the kinetic influence of specific residues on protein carbonylation, we used the GB1 protein as a model. The wide-type (WT) GB1 contains no Cys residue that is a highly reactive sulfur-containing residue and a key player in the 4-HNE induced protein oxidization and polymerization. Therefore, to explore the kinetics of the protein oxidization, we also implemented site-directed mutagenesis to introduce Cys substitutions at two distinct positions within the GB1 protein: Lys 28 (K28C GB1) and Thr 53 (T53C GB1), residing at the α-helical and β-sheet regions, respectively. These two sites were selected to represent different structural environments within the protein, enabling comparative analysis of multi-step oxidation kinetics and the contributions of active amino acids and structures.

To elucidate the protein carbonylation and oligomerization induced by 4-HNE at the molecular level, we set to track the reacting systems using solution-state NMR. We used the full chemical shift assignments of GB1 that were reported previously by several studies to assign ^{1}H-^{15}N HSQC spectrum. The reactions of GB1 proteins interacting with 4-HNE were tracked by recording the ^{1}H-^{15}N HSQC spectra at a serial of time points after adding 4-HNE. As demonstrated in Figure 2, the NMR signals remain very similar for WT GB1 during the initial hours of reacting with 4-HNE, indicating that the protein structure remained unchanged. Reduced NMR signal intensities were observed in 3-6 days for several residues such as T44, T53 and T17, and the majority of the signals disappeared after 33 days. Notably, no significant chemical shift perturbations were observed, suggesting the overall protein structure remained largely unchanged. The reduction and eventual disappearance of signals indicate the formation of GB1 oligomers, likely through 4-HNE-mediated cross-linking, a process that progresses over time. Residues affected by this reaction and/or oligomerization are highlighted in Figure 2D. In contrast to WT GB1, as shown in Figure 2B, T53C GB1 reacting with 4-HNE started within the first few hours. The continuous peak intensity attenuation was observed for many residues afterwards, and most peaks became absent at Day 10, inferring that the reactions led to the cross-linking of proteins by 4-HNE and the formation of large oligomers over time. Similarly, peaks in the ^{1}H-^{15}N HSQC spectra of K28C GB1 underwent changes upon adding 4-HNE (Figure 2C), however, to a less extent in comparison with the case of T53C GB1. Signal intensity reduction was observed for several residues within the first few hours, continuing to progress over time. After 10 days, almost all peaks disappeared, indicating the formation of large oligomers. The formation of oligomers was also confirmed by MALDI-TOF mass spectrometry (one example is demonstrated in Figure 2D as discussed below). The NMR results suggest that the generation rate of protein carbonylation induced by 4-HNE is mostly driven by the active groups, such as, thiol groups of cysteine residues, which in turn to trigger reactions of other residues, tend to cross-link GB1 monomers to form an oligomeric network, rather than producing more carbonylated proteins. Although WT GB1 lacks thiol-driven reactions, the hydroxyl (R-OH) and amino ($R\text{-}NH_2$) groups on residues like Thr and Lys can still react slowly with 4-HNE, eventually leading to the formation of oligomers. The increase sizes of these oligomers resulted in the decrease in signal intensity in NMR spectra. Furthermore, the specific affected residues and the rate of signal intensity reduction differ between K28C and T53C GB1, indicating that oligomerization depends on the location of cysteine residues and the overall protein structure. These results suggest a correlation

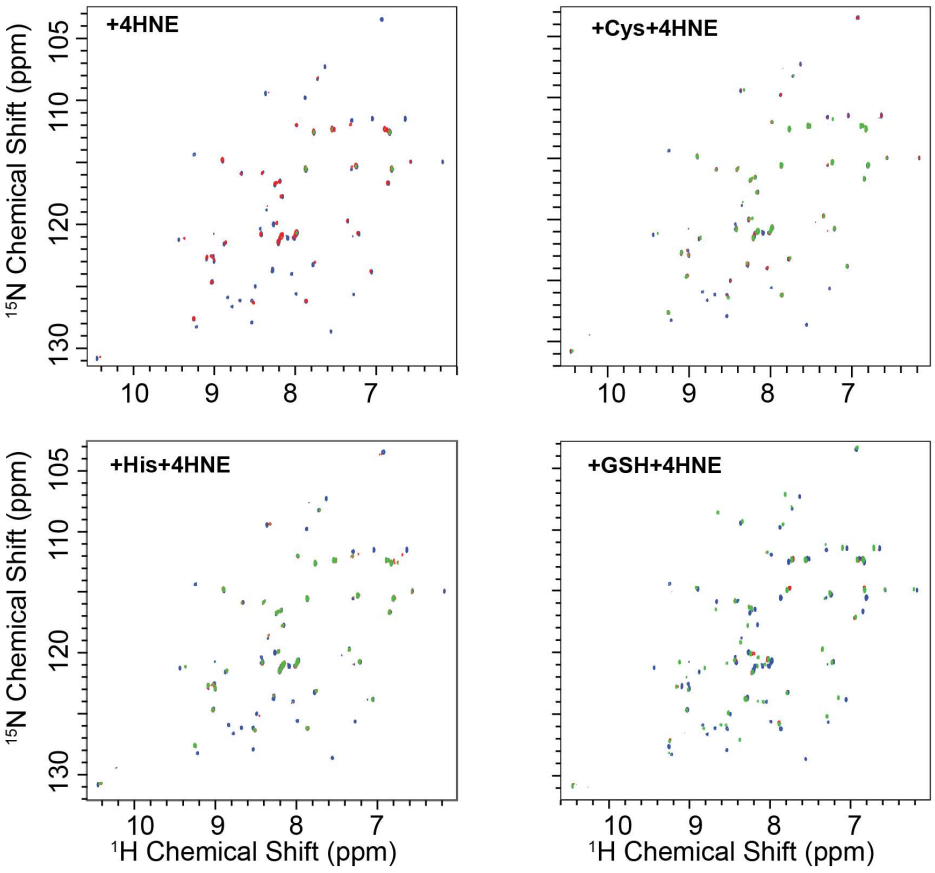

Figure 3. ^{1}H-^{15}N HSQC NMR spectra of T53C GB1 reacting with 4-HNE with or without Cys, His, and GSH. The spectra were recorded on the time points of 0 (blue), 6 hours (red) and 7 days (green) of the reactions. The T53C GB1 concentrations were 1.6 mg/ml, and the 4-HNE, Cys, His, and GSH concentrations were all 10 mM. It is noted that after adding GSH, many GB1 NMR peaks were slightly shifted due to the pH change introduced by the addition of GSH as shown in the bottom right graph.

between the yellowing of the solution and the progressive, 4-HNE cross-link-mediated oligomerization of GB1.

3.3 Inhibitors attenuating the protein oxidation and oligomerization resolve skin yellowness.

To further elucidate the underlying mechanisms, we set to explore the impacts of several potential inhibitors (Cys, His, and GSH) on GB1 proteins reacting with 4-HNE by NMR spectroscopy. T53C GB1 was chosen in this investigation as it was more reactive than the other variants as discussed above. NMR experiments were conducted to characterize the effects of inhibitors. As displayed in Figure 3, the ^{1}H-^{15}N HSQC NMR signals of T53C GB1 largely disappeared after 7-day reaction with 4-HNE due to the formation of oligomers for T53C GB1. When adding Cys, His or GSH in the reaction systems, the majority of the NMR signals were still present. The NMR study further illustrated that the three molecules inhibit 4-

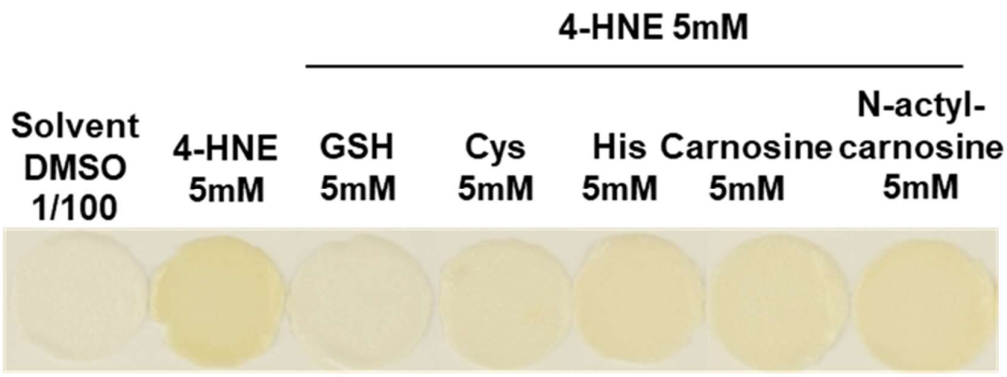

Figure 4. Inactive reconstructed skin model was exposed to 4HNE and quenchers for 7 days in 37°C

HNE induced T53C GB1 oligomerization. In addition, Cys appears exhibiting slightly stronger attenuation effects than His on the protein oligomerization based on NMR data.

We next performed experiments with skin models to elucidate whether the observed inhibiting effects still hold in the corresponding cases. As displayed in Figure 4, the inhibitory effects of Cys,His,GSH on the protein oligomerization are indeed consistent with the NMR experiments.In contrast,treatment with GSH resulted in a substantial reduction in yellowing on the 3D skin model shown in Figure 4. This enhanced efficacy of GSH may be attributed to its facile reactivity with 4-HNE in neutral solutions, whereas the reaction of Cys with 4-HNE is reportedly more complex, usually requiring excess Cys for thiazolidine derivative formation [17]. And we also tested the carnosine and N-actyl-carnosine which all containing histidine chemistry structure. The carnosine showed inhibitory effect but N-actyl-carnosine not.

4.Discussion

The phenomenon of protein carbonylation, characterized by the irreversible addition of carbonyl groups to proteins, is chiefly mediated by reactive aldehydes such as 4-HNE, a byproduct of lipid peroxidation under oxidative stress conditions. This modification drastically alters the structure and function of key skin proteins, including collagen and elastin, leading to hallmark signs of aging skin such as increased wrinkling, reduced elasticity, and impaired barrier function.

This study elucidates the relationship between protein carbonylation and skin yellowness, for the first time provided the direct evidence of protein discoloration due to carbonylation and subsequential reactions and explored the underlying chemical mechanisms. Futhermore,skin yellowness, a complex manifestation of skin aging, involves both chemical reactions of protein modification and biological alterations due to protein dysfunction. Understanding of the biological pathways involved, particularly the role of reactive aldehydes like 4-HNE, a byproduct of lipid peroxidation, in inducing carbonyl modifications that lead to yellowish changes in skin, offers valuable insights for mitigating aging. It also indicated that protein carbonyls could be serve as a kind of biomarker for skin aging relate to protein homeostasis. These findings provided new insights for the development of novel strategies for preventing and improvingskin aging yellowness.

5.Conclusion

The molecular mechanisms of 4-HNE, as a presentitave reactive aldehydes, reacting with proteins revealed by this study showed that protein carbonylation and the subsequent cross-linking reactions might be an important contributor to skin aging yellowness These cross-linked protein products may alter light absorption or scattering in skin, resulting in a yellowish appearance. Therefore, not only protein carbonyls is a critical indicator of aging, but also the subsequential olimerization of proteins generated yellowish products. To effectively mitigate this phenomenon, in addition to preventative strategies targeting lipid oxidation, such as preventing from sun exposure and ozone and antioxidation, strategies targeting reactive aldehydes, such as scavenging by nucleophilic compounds, are also effective approaches. As shown in this study, thiol-containing compounds such as cysteine and GSH and specific amino acids such as hisditine, can effectively inhibit protein cross-link, and may offer as promising approaches to address skin aging yellowness.

6.References

[1] Y. Lu, J. Yang, K. Xiao, M. Pointer, C. Li, and S. Wuerger, “Skin coloration is a culturally-specific cue for attractiveness, healthiness, and youthfulness in observers of Chinese and western European descent,” *PLoS One*, vol. 16, no. 10 October, pp. 1–17, 2021, doi: 10.1371/journal.pone.0259276.

[2] R. R. Anderson, R. R. Anderson, J. A. Parrish, and J. A. Parrish, “The Optics of Human Skin,” *J. Invest. Dermatol.*, 1981, doi: 10.1111/1523-1747.ep12479191.

[3] B. L. Lua and J. Robic, “Yellowness in skin complexion: Analysis of self-perception of women in China evaluated against clinical parameters of yellowness,” *Ski. Res. Technol.*, vol. 30, no. 8, pp. 1–14, 2024, doi: 10.1111/srt.13831.

[4] Y. Nishimori, A. D. Pearse, C. Edwards, and R. Marks, “Elastotic degenerative change and yellowish discolouration in photoaged skin,” *Ski. Res. Technol.*, vol. 4, no. 2, pp. 79–82, 1998, doi: 10.1111/j.1600-0846.1998.tb00090.x.

[5] H. Ohshima *et al.*, “Melanin and facial skin fluorescence as markers of yellowish discoloration with aging,” *Ski. Res. Technol.*, vol. 15, no. 4, pp. 496–502, 2009, doi: 10.1111/j.1600-0846.2009.00396.x.

[6] F. Yi *et al.*, “A cross-sectional study of Chinese women facial skin status with environmental factors and individual lifestyles,” *Sci. Rep.*, vol. 12, no. 1, pp. 1–14, 2022, doi: 10.1038/s41598-022-23001-6.

[7] L. M. Ashton, K. B. Pezdirc, M. J. Hutchesson, M. E. Rollo, and C. E. Collins, “Is skin coloration measured by reflectance spectroscopy related to intake of nutrient-dense foods? A cross-sectional evaluation in Australian young adults,” *Nutrients*, vol. 10, no. 1, 2018, doi: 10.3390/nu10010011.

[8] B. Gondal and A. Aronsohn, “A Systematic Approach to Patients with Jaundice,” *Semin. Intervent. Radiol.*, vol. 33, no. 4, pp. 253–258, 2016, doi: 10.1055/s-0036-1592331.

[9] B. Fang *et al.*, “A Potential Role of Keratinocyte-Derived Bilirubin in Human Skin Yellowness and Its Amelioration by Sucrose Laurate/Dilaurate,” *Int. J. Mol. Sci.*, vol. 23,

no. 11, 2022, doi: 10.3390/ijms23115884.

[10] V. Haydont, B. A. Bernard, and N. O. Fortunel, “Age-related evolutions of the dermis: Clinical signs, fibroblast and extracellular matrix dynamics,” *Mech. Ageing Dev.*, vol. 177, no. March 2018, pp. 150–156, 2019, doi: 10.1016/j.mad.2018.03.006.

[11] Q. Li *et al.*, “Assessing the Role of Carbonyl Adducts, Particularly Malondialdehyde Adducts, in the Development of Dermis Yellowing Occurring during Skin Photoaging,” *PLoS One*, vol. 10, no. 3, pp. 1–14, 2022, doi: 10.3390/life12030403.

[12] H. Zucchi, H. Pageon, D. Asselineau, M. Ghibaudo, I. Sequeira, and S. Girardeau-Hubert, “Assessing the Role of Carbonyl Adducts, Particularly Malondialdehyde Adducts, in the Development of Dermis Yellowing Occurring during Skin Photoaging,” *Life*, vol. 12, no. 3, 2022, doi: 10.3390/life12030403.

[13] B. Coffaro and C. P. Weisel, “Reactions and Products of Squalene and Ozone: A Review,” *Environ. Sci. Technol.*, vol. 56, no. 12, pp. 7396–7411, 2022, doi: 10.1021/acs.est.1c07611.

[14] H. C. H. Yeo and T. Shibamoto, “Formation of formaldehyde and malonaldehyde by photooxidation of squalene,” *Lipids*, vol. 27, no. 1, pp. 50–53, 1992, doi: 10.1007/BF02537059.

[15] K. J. Dennis and T. Shibamoto, “Gas chromatographic analysis of reactive carbonyl compounds formed from lipids upon UV-irradiation,” *Lipids*, vol. 25, no. 8, pp. 460–464, 1990, doi: 10.1007/BF02538089.

[16] B. Fang, L. Li, J. Winget, T. Laughlin, and T. Hakozaki, “Identification of Yellow Advanced Glycation End Products in Human Skin,” *Int. J. Mol. Sci.*, vol. 25, no. 11, 2024, doi: 10.3390/ijms25115596.

[17] H. Esterbauer, “Estimation of peroxidative damage. A critical review,” *Pathol. Biol.*, vol. 44, no. 1, pp. 25–28, 1996.